Proceedings of the ASME 2018 International Mechanical Engineering Congress and Exposition
IMECE 2018
November 9-15, 2018, Pittsburgh, PA, USA

IMECE2018-87742

DRAFT: HYPO/HYPERGLYCEMIC CONSTRAINED DESIGN OF IV INSULIN CONTROL FOR TYPE 1 DIABETIC PATIENTS WITH MEAL AND INITIAL CONDITION UNCERTAINTIES USING SEQUENTIAL QUADRATIC PROGRAMMING

Souransu Nandi
Control, Dynamics and Estimation Laboaratory
Department of Mechanical and Aerospace Engineering
University at Buffalo
Buffalo, New York 14260
Email: souransu@buffalo.edu

Tarunraj Singh
Control, Dynamics and Estimation Laboaratory
Department of Mechanical and Aerospace Engineering
University at Buffalo
Buffalo, New York 14260
Email: tsingh@buffalo.edu

ABSTRACT

The focus of this paper is on the development of an open loop controller for type 1 diabetic patients which is robust to meal and initial condition uncertainties in the presence of hypo- and hyperglycemic constraints. Bernstein polynomials are used to parametrize the evolving uncertain blood-glucose. The unique bounding properties of these polynomials are then used to enforce the desired glycemic constraints. A convex optimization problem is posed in the perturbation space of the model and is solved repeatedly to sequentially converge on a sub-optimal solution. The proposed approach is demonstrated on the classic Bergman model for Type 1 diabetic patients.

1 INTRODUCTION

In 2015, a report released by the Centers for Disease Control and Prevention (CDC) on the National Diabetes Statistics revealed that a significant 30.3 million people in United States alone have diabetes, which accounts for about 9.4% of the US population [1]. Moreover, WHO reported that there has also been a staggering rise in the growth of diabetes worldwide where the number of people with diabetes has risen from 108 million in 1980 to 422 million in 2014 [2]. This is clearly a worldwide epidemic with the cost to health care being enormous. These numbers are expected only to rise in the future unless substantial progress is made in diabetes research to solve or even mitigate the impact of uncontrolled blood-glucose.

The natural control of blood glucose concentration level is primarily facilitated by two hormones (namely the glucagon and the insulin), both of which are secreted by the pancreas. This loss of glucose regulation due to autoimmune diabetes (Type 1) or insulin-resistant diabetes (Type 2) can have dire health consequences. For individuals with diabetes, the undesirable events where the blood glucose level rises above the 180 mg/dL mark and falls below the 70 mg/dL mark are called hyperglycemia and hypoglycemia respectively. Critical hypoglycemia (glucose $<$ 50 mg/dL) can lead to seizures, unconsciousness as well as possible permanent brain damage [3] while chronic hyperglycemia can lead to blindness, nerve damage and potential loss of limbs; thereby emphasizing the severity of the ailment in discussion.

In response to the alarming rise in Diabetes the Juvenile Diabetes Research Foundation launched a consortium in 2006 [4] and the European Union initiated the AP@Home effort in 2010 [5], to promote the development of an *Artificial Pancreas* (AP). AP is a bio-medical device which integrates an insulin pump along with a glucose sensor to mimic the operations of a natural pancreas.

Cobelli et al. in [4] review the history of the effort to develop an *Artificial Pancreas (AP)* (also referred to as a *bionic pancreas* [6] or an *artificial β cell* [7]). Lunze et al. [8] reviewed the current state of controllers proposed for use in automated blood glucose regulation. Dassau et al. [7] makes comparisons of

different algorithms to detect meal times using continuous glucose measurement (CGM) from 26 children. It is observed in the datasets that significant variation of baseline glucose level exists. Moreover, remarks are also made on the uncertainty in meal quantities (in terms of carbohydrates). Both of these variables have been considered as uncertain in this paper. Chen et al. [9] also remark on the meal detection challenge due to meal macronutrient composition uncertainty and variation in patient specific physiology.

With the advent of sensing technology and sophisticated insulin pumps, the goal of closed loop glycemic control today is almost a reality. However, there remains a significant number of obstacles that needs attention; one of which is addressed in this paper. Particularly, that of the design of an insulin control algorithm that addresses the impact of initial condition and meal-size uncertainties.

This paper is an attempt to develop a framework to characterize the uncertainty in the evolution of blood glucose due to various sources of uncertainties and determine an open loop control trajectory that can deal with them. In this paper we consider two such sources: uncertainty in the initial conditions (blood glucose) and uncertainty in the meal size (number of carbohydrates in the meal). A spectral expansion based approach to represent the evolution of blood glucose uncertainty is proposed and special properties of its bases (Bernstein polynomials) are used to determine bounds on the range of variation. These bounds are then utilized to solve for a control strategy that forces the uncertainty in glucose to meet certain constraints as well as track the blood glucose level of a normal person. The final optimization problem thus formed is iteratively solved by formulating a convex optimization problem repeatedly, to converge to a reasonable solution.

This document is organized as follows. Section 1 motivates & introduces the problem statement, provides existing background literature and presents a brief summary of the work in this paper. Section 2 talks about the Bergman model for glucose-insulin dynamics and describes the simulation environment. Section 3 reviews the well-known Galerkin Projection technique to determine coefficients of a series expansion of stochastic states. Section 4 presents Bernstein polynomials and motivates their choice as basis functions for a series expansion. Section 5 gives a detailed account of the Sequential Quadratic Programming algorithm that has been used to solve an optimal control problem. Finally, the paper ends with concluding remarks in section 6.

2 MODEL AND SIMULATION ENVIRONMENT

2.1 Dynamic Model

The control design in this work has been implemented on the popular Bergman's Minimal model for glucose-insulin dynamics [10], although the strategy can be easily adapted for more sophisticated models. The minimal model is a two compartment physiological model where the evolution of the model states are defined by

$$\dot{G}(t) = -(X(t) + p_1)G(t) + p_1 G_b + D(t) \tag{1}$$

$$\dot{X}(t) = -p_2 X(t) + p_3(I(t) - I_b) \tag{2}$$

$$\dot{I}(t) = \begin{cases} -p_4 I(t) + \gamma(G(t) - h)(t - t_m) & \text{for } t \geq t_m \text{ and} \\ & G(t) \geq h \\ -p_4 I(t) & otherwise \end{cases} \tag{3}$$

p_1 (min^{-1}), p_2 (min^{-1}), p_3 $(min^{-2}.L/mU)$, p_4 (min^{-1}), γ $(min^{-2}.mU.dL/mg.L)$ and h (mg/dL) are parameters of the model. The states $G(t)$ (mg/dL), $X(t)$ (min^{-1}) and $I(t)$ (mU/L) represent the blood (plasma) glucose concentration, (effective) insulin in the remote compartment and the plasma insulin concentration respectively.

G_b and I_b represent certain basal values of the states $G(t)$ and $I(t)$. The term $\gamma(G(t) - h)(t - t_m)$ mimics the action of the human pancreas, t_m (which has been assumed to be $30\,min$ for all simulations) is time of meal consumption.

The additional term $D(t)$ is introduced in the model to replicate a meal intake disturbance. In this work, the structure of the meal disturbance ($D(t)$) is assumed to be that defined by Fisher in [11] as

$$D(t) = \begin{cases} 0 & t < t_m \\ Be^{-d(t-t_m)} & t \geq t_m \end{cases}$$

where d is the natural rate of decay of glucose in blood and B characterizes the quantity of food consumed. To make $D(t)$ a smooth function (as opposed to piecewise continuous), it is written in terms of a sigmoidal function as

$$D(t) = Be^{-d(t-t_m)}\left(1 - \frac{1}{1 + e^{r(t-t_m)}}\right) \tag{4}$$

where r defines the steepness of the sigmoid part (and is chosen to be $r = 100$ for all simulations).

One of the objectives of the control problem is to make the glucose concentration in a Type 1 diabetic patient track the glucose concentration of a normal person over time after a meal. The variation of glucose concentration for a normal person is referred to as the target glucose trajectory. This target trajectory is generated by simulating the Bergman's model using parameter values fitted to a normal person along with a gut dynamics model adopted from [12]. The reason a higher order model was selected was for the generation of a realistic nominal target trajectory. A

lower order model for the controller design was strictly for illustrative purposes. Since these parameters vary among people, a set of values are chosen, for illustrative purposes, from literature [13, 14]; where the Bergman model and the gut dynamics were actually fit to real data (taken from a normal subject(s)). The pertinent parameters and details regarding the gut dynamics model can be found in the Appendix Section.

It should be noted that during practical implementation, the parameters and initial conditions are not binding and can be altered depending on the target trajectory desired for a patient. In fact, the target trajectory need not be obtained from a model simulation and could be prescribed by the respective physician. However, in this work as mentioned previously, for illustration, the target trajectory is obtained from a simulation.

In case of a person suffering from Type-1 diabetes, the natural pancreas ($\gamma(G(t)-h)(t-t_m)$) is removed and is substituted by an artificial insulin input term $U'(t)$ similar to Lynch and Bequette in [15]. This alters equation (3) to

$$\dot{I}(t) = -p_4 I(t) + U'(t). \tag{5}$$

The diabetic model (comprised of equations (1), (2) and (5)) is now an unstable system in the absence of any insulin control causing the glucose concentration to grow unchecked (which is reasonable to assume: for a Type 1 diabetic patient with no insulin). To stabilize the glucose concentration in such patients, in reality, a basal insulin dosage is given. This concept can be modeled by assuming the control to be of the form

$$U'(t) = U(t) + p_4 I_b \tag{6}$$

where the term $p_4 I_b$ mimics the basal dosage. With this modification, the diabetic model can be summarized as

$$\dot{G}(t) = -(X(t) + p_1)G(t) + p_1 G_b + D(t) \tag{7}$$

$$\dot{X}(t) = -p_2 X(t) + p_3 (I(t) - I_b) \tag{8}$$

$$\dot{I}(t) = -p_4 (I(t) - I_b) + U(t). \tag{9}$$

Equations (7) through (9) now represent a stable system where the glucose concentration is driven to the desired basal level (G_b).

The values for the parameters (corresponding to Type-1 diabetic patients) are chosen from literature [15] and are given by

$$p_1 = 0.028735 \ \frac{1}{min};\ p_2 = 0.028344 \ \frac{1}{min}; \tag{10}$$

$$p_3 = 5.035e-5 \ \frac{mU}{L};\ p_4 = \frac{5}{54} \ \frac{1}{min};\ d = 0.05. \tag{11}$$

The basal values for plasma glucose and insulin concentrations were obtained by averaging respective values from 30 subjects (10 of each: adults, adolescents and children) available from the FDA approved Type 1 Diabetes Metabolic Simulator (T1DMS) software. These values are

$$G_b = 119.1858 \ \frac{mg}{dL} \ \text{ and } \ I_b = 15.3872 \ \frac{mU}{L}. \tag{12}$$

In this work, it is assumed that the initial value of glucose concentration in plasma ($G(0)$ or G_0) and the meal quantity (B) are uncertain variables with known specific distributions.

2.2 Distribution of G_0 and B

Since the initial value of blood glucose concentration (G_0) is unlikely to be exactly the basal value (G_b), G_0 is assumed to be uniformly distributed about G_b with a 30% variation on either side of it. Therefore, $G_0 \in U[83.43, 154.9415]$. It can be defined in terms of another uniformly distributed random variable (ξ_1) where $\xi_1 \in U[0,1]$ as

$$G_0 = 0.7G_b + (2 \times 0.3)G_b \xi_1. \tag{13}$$

According to the 2010 Dietary Guidelines [16] published by the U. S. Department of Agriculture, Health and Human Services, the daily carbohydrate (CHO) intake goal for all ages should be 130 gr. Depending on the individual and time of day, meal sizes can vary. Light and heavy meals vary in their CHO counts significantly. The values can vary between 15 gr for a snack to 75 gr for lunch if CHOs from all foods at a meal are added up. A breakdown of the carbohydrate content of recommended foods for diabetic patients can be found in the article [17] from the American Diabetes Association. Based on the daily total and mealtime CHO recommedations, a meal of 45 gr of CHO is assumed to be common practice. Hence, a beta distribution is assumed for the meal quantity with its mode corresponding to a meal of 45 gr of CHO.

To determine the value of B corresponding to a 45 gr CHO meal, the glucose appearance rate in plasma ($Ra_g(t)$) was observed from a T1DMS simulation (for an average adult subject). The area under the curve Ra_g was evaluated to estimate the total concentration of glucose that was absorbed in the plasma. Consequently, B was chosen such that the area under the curve $D(t)$ was the same as the area under the curve Ra_g ensuring that the same amount of glucose entered the blood stream (in the Bergman model) as deemed acceptable by the FDA.

Table. 1 shows the values of B determined for 3 different quantities of meals. Based on these numbers, the random variable B

	30 gr	45 gr	60 gr
B	19.46	28.98	38.91

TABLE 1. Values of B for different meal sizes

is expressed as an affine function of a Beta random variable (ξ_2), where ξ_2 is defined over $[0,1]$ with parameters $\alpha = 7$ and $\beta = 5$. The expression of B is written as

$$B = 48\xi_2. \tag{14}$$

With this distribution, B has a mode at $B = 28.8$, which is very close to B corresponding to a 45 gr CHO meal (Table. 1) as seen in Figure. 1.

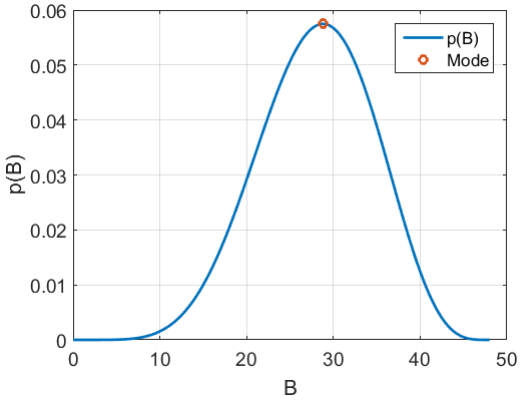

FIGURE 1. Distribution of B

3 GALERKIN PROJECTION

If the model is observed carefully, it can be seen that $X(t)$ and $I(t)$ can be solved independently from $G(t)$. Moreover, since the uncertainties are only with B and G_0; $X(t)$ and $I(t)$ can be solved deterministically making $G(t)$ the only evolving stochastic state. In this work, the stochastic $G(t)$ state is approximated by a finite series expansion (similar to a Polynomial Chaos Expansion of the glucose state in [18]) as follows

$$\hat{G}(t) = \sum_{i=0}^{N} x_i(t)\Psi_i(\xi_1,\xi_2) \tag{15}$$

where $x_i(t)$ are the time varying coefficients of the basis functions $\Psi_i(\xi_1,\xi_2)$ (typically selected to be a special polynomial basis set) and N is the order of expansion desired. The goal is to determine $x_i(t)$ so that the glucose concentration at any instant in time can be known as a polynomial function of the uncertain variables ξ_1 and ξ_2.

Galerkin Projection allows the determination of these coefficients $x_i(t)$ by forming a deterministic set of coupled differential equations. This is done by minimizing the expected value of the approximation error square over the uncertain space. An illustration on the problem at hand is shown below.

The objective of the Galerkin Projection is to determine $x_i(t)$ such that

$$J = \int_0^1 \int_0^1 (\dot{G} - \dot{\hat{G}})^2 pdf(\xi_1)pdf(\xi_2)d\xi_1 d\xi_2 \tag{16}$$

is minimized. Deriving the necessary conditions for the minima leads to $N+1$ differential equations

$$\frac{\partial J}{\partial x_i} = \int_0^1 \int_0^1 (\dot{G} - \dot{\hat{G}})\Psi_i pdf(\xi_1)pdf(\xi_2)d\xi_1 d\xi_2 = 0. \tag{17}$$

Recognizing the weighted inner product operator

$$\langle f(\xi_1,\xi_2), g(\xi_1,\xi_2)\rangle = \int_0^1 \int_0^1 (f)(g)pdf(\xi_1)pdf(\xi_2)d\xi_1 d\xi_2, \tag{18}$$

equation (17) can be simplified to

$$\underbrace{\begin{bmatrix} \dot{x_0} \\ \dot{x_1} \\ \vdots \\ \dot{x_N} \end{bmatrix}}_{\boldsymbol{X_G}} = \underbrace{\begin{bmatrix} \langle\Psi_0,\Psi_0\rangle & \dots & \langle\Psi_0,\Psi_N\rangle \\ \langle\Psi_1,\Psi_0\rangle & \dots & \langle\Psi_1,\Psi_N\rangle \\ \vdots & \ddots & \vdots \\ \langle\Psi_N,\Psi_0\rangle & \dots & \langle\Psi_N,\Psi_N\rangle \end{bmatrix}^{-1} \begin{bmatrix} \langle f_G,\Psi_0\rangle \\ \langle f_G,\Psi_1\rangle \\ \vdots \\ \langle f_G,\Psi_N\rangle \end{bmatrix}}_{\boldsymbol{F_G}(t)} \tag{19}$$

where f_G is the right hand side of equation (7) and $\boldsymbol{X_G} \in \mathbb{R}^{N+1}$ is a vector comprising all the time varying coefficients of expansion. Solutions of equation (19) now yields $x_i(t)$ over time and allows us to evaluate the blood glucose concentration as a polynomial function of the uncertain variables for any realization. However, in order to do so, first an appropriate set of basis functions Ψ_i needs to be selected. The next section presents and motivates a well known bases in the form of Bernstein polynomials.

4 BERNSTEIN POLYNOMIALS

In numerous fields of engineering, it is often desired to determine the bounds on the range of a particular state or function.

If the particular function of interest is, or can be well approximated by a multivariate polynomial, Bernstein polynomials can be exploited to determine these bounds [19]. In fact, algorithms have also been proposed to determine the exact range of multivariate polynomials [20] using Bernstein expansions. The work presented here, however, makes use of the bounding properties of Bernstein bases to estimate tight bounds on the range of stochastic states and use these bounds as constraints to design a robust controller.

Since there are only 2 uncertain variables considered in this paper, the bounding property corresponding to bi-variate Bernstein polynomials is summarized below. If a polynomial function of ξ_1 and ξ_2 ($z(\xi_1,\xi_2)$) is expressed in terms of Bernstein polynomial basis functions ($B^d_{\xi_1,\xi_2}(\xi_1,\xi_2)$) as

$$z(\xi_1,\xi_2) = \sum_{\xi_1,\xi_2=0}^{d,d} b_{\xi_1,\xi_2} B^d_{\xi_1,\xi_2}(\xi_1,\xi_2) \tag{20}$$

where $B^d_{\xi_1,\xi_2}(\xi_1,\xi_2) = \prod_{i=1}^{2} B^d_{\xi_i}(\xi_i)$ are the bi-variate Bernstein polynomials (developed using a tensor product of univariate Bernstein polynomials ($B^d_{\xi_i}(\xi_i)$) with degree d) and b_{ξ_1,ξ_2} are the Bernstein coefficients; the range enclosing property of Bernstein polynomials over the box $[\xi_1,\xi_2]^T = \boldsymbol{\xi} = [0,1]^2$ is given by

$$z(\boldsymbol{\xi}) \subseteq \Big[\min_{\xi_1,\xi_2=0}^{d,d} b_{\xi_1,\xi_2}, \max_{\xi_1,\xi_2=0}^{d,d} b_{\xi_1,\xi_2}\Big]. \tag{21}$$

Expression (21) can now be used to immediately obtain bounds on z, i.e. get an upper bound and a lower bound on the magnitude of the polynomial in the domain $\boldsymbol{\xi} = [0,1]^2$.

This unique range enclosing property now motivates us to choose the basis functions in equation (15) as Bernstein polynomials, i.e. we assume

$$\Psi_0 = B^d_{0,0}(\xi_1,\xi_2); \ldots; \Psi_N = B^d_{d,d}(\xi_1,\xi_2). \tag{22}$$

Such an expansion would now allow us to easily determine the upper (G_{ub}) and lower bounds (G_{lb}) of the stochastic Glucose state ($\hat{G}(t)$) at any instant in time using the relations

$$G_{lb}(t) = min(x_0(t), x_1(t), \ldots, x_N(t)) \tag{23}$$

$$G_{ub}(t) = max(x_0(t), x_1(t), \ldots, x_N(t)) \tag{24}$$

if the variation of $x_i(t)$ were known over time. A comprehensive system can be defined by augmenting the system in equation (19) by the two other remaining states of the Bergman model (i.e. X and I). This leads to the system of differential equations given by

$$\underbrace{\begin{bmatrix} \dot{\boldsymbol{X}}_{\boldsymbol{G}} \\ \dot{X} \\ \dot{I} \end{bmatrix}}_{\dot{\boldsymbol{X}}} = \underbrace{\begin{bmatrix} \boldsymbol{F}_{\boldsymbol{G}} \\ f_X \\ f_I \end{bmatrix}}_{\boldsymbol{F}} \tag{25}$$

where

$$\hat{G}(t) = [\Psi_0, \ldots, \Psi_N, 0, 0] \times \boldsymbol{X}(t) \tag{26}$$

and $\boldsymbol{X} \in \mathbb{R}^{N+3}$ is a vector comprising all the states necessary to accurately determine the statistics of $\hat{G}(t)$ as well as the bounds on $\hat{G}(t)$.

In order to simulate equation (25), we need to know the initial conditions of the system (i.e. $\boldsymbol{X}(0)$). It is assumed that the terminal two states (X and I) at time $t = 0$ is at their steady state values ($X(0) = 0$ and $I(0) = I_b$) which is not an unreasonable supposition. The initial condition for $x_i(0)$, however, needs to be determined specially since the relation $G(0) = \hat{G}(0)$ has to be satisfied. $G(0)$ as well as $\hat{G}(0)$ are both polynomial functions in ξ_1 and ξ_2. Therefore a linear mapping (M_0) can be found to determine $x_i(0)$ from the polynomial coefficients of equation (13) by comparing coefficients, i.e. since we have

$$G(0) = \hat{G}(0) \tag{27}$$

$$\Rightarrow [1, \xi_1] \begin{bmatrix} 0.7G_b \\ 0.6G_b \end{bmatrix} = \underbrace{[\Psi_0, \ldots, \Psi_N]}_{\Psi} \begin{bmatrix} x_0(0) \\ \vdots \\ x_N(0) \end{bmatrix} \tag{28}$$

we can compare coefficients of the two polynomials to get

$$\begin{bmatrix} x_0(0) \\ \vdots \\ x_N(0) \end{bmatrix} = M_0 \begin{bmatrix} 0.7G_b \\ 0.6G_b \end{bmatrix}. \tag{29}$$

Now that $\boldsymbol{X}(0)$ is known, system in equation (25) can be simulated.

Figure 2 illustrates the results of numerical simulations. Figure 2 is generated using values of $d = 4$ leading to a value of $N = 24$ (i.e. a total of 25 basis functions were selected in the series expansion). The black plots show the upper and lower bounds determined using relations (23) and (24). To confirm

the bounds are sound, 10000 Monte Carlo (MC) simulations are done for different realizations of ξ_1 and ξ_2. It is evident from the figure that the determined Bernstein bounds successfully envelop all those samples.

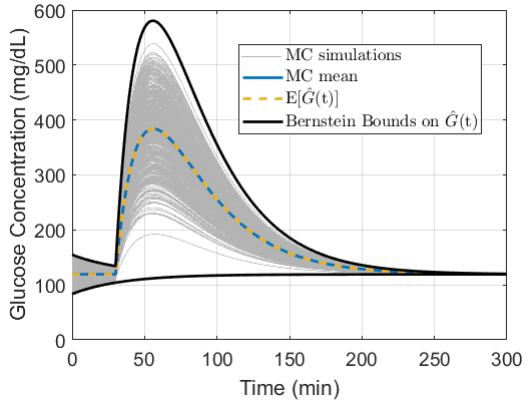

FIGURE 2. Comparison of MC mean with E[$\hat{G}$(t)] and Bernstein Bounds

The figure also compares how well the mean is captured by the coefficients $x_i(t)$. The mean trajectory can be evaluated using the relation

$$E[\hat{G}(t)] = x_0 E[\Psi_0] + \ldots + x_N E[\Psi_N] \tag{30}$$

$$= \underbrace{[E[\Psi_0], \ldots, E[\Psi_N]]}_{M_{mean}} \boldsymbol{X_G}. \tag{31}$$

The blue curve is the mean trajectory determined from the 10000 MC realizations and the dotted yellow curve is the mean trajectory determined using equation (31). Once again it is evident that the information necessary to construct the mean trajectory is well captured by the evolving coefficients $x_i(t)$. It should be noted that the IV insulin control profile assumed during the simulation is $U(t) = 0$.

Now that a method of characterizing and quantifying the uncertainty in the glucose state has been established, a control strategy can be developed to address the robust optimal control problem as seen in the subsequent section.

5 SEQUENTIAL QUADRATIC PROGRAMMING

This section of the paper gives a detailed outline of the optimal control problem and the methodology used to solve it. It should be stated that the final solution being sought is that of an open loop control profile ($U^*(t)$) which makes the mean glucose trajectory ($E[\hat{G}(t)]$) track a target trajectory ($G_{target}(t)$) as closely as possible while simultaneously ensuring that at no instant in time does any sample trajectory (i.e. a stochastic realization) violate certain pre-determined constraints. The nature of these constraints have been elaborated below.

It is recommended that plasma glucose concentration never falls below a lower bound G_{dlb} (hypoglycemia) at any time. According to a joint consensus statement from the ADA and the Endocrine Society regarding hypoglycemia and diabetes [21], G_{dlb} should be $70\frac{mg}{dL}$. In addition, after two hours ($120\,min$) of a meal, it is recommended by the American Diabetes Association [22] that the plasma glucose concentration be below $180\,\frac{mg}{dL}$.

To meet all these goals, an optimal control problem ($P1$) can be posed as follows

$$\begin{aligned} \text{minimize}_{U(t)} \quad & \int_0^{T_f} (E[\hat{G}(t)] - G_{target}(t))^2 dt \\ \text{subject to} \quad & \hat{G}(t,\xi_1,\xi_2) \geq G_{dlb} \text{ for } t \geq 0 \\ & \hat{G}(t,\xi_1,\xi_2) \leq G_{dub} \text{ for } t \geq t_m + 120 \\ & U(t) \geqslant 0 \\ & \text{for any } \xi_1 \subset [0,1] \text{ and } \xi_2 \subset [0,1] \end{aligned} \tag{32}$$

whose solution yields $U^*(t)$. Solving the problem described in equation (32) is the main goal of this paper. It is a non-linear non-convex optimization problem in the continuous time domain. Therefore, to seek a solution, in this work, the problem is first approximated by another surrogate equivalent optimization problem (in the discrete time domain) which is convex ($P2$). Then an algorithm which solves $P2$ repeatedly to sequentially converge on a sub-optimal solution to $P1$ is exercised. The development of $P2$ and the algorithm is what comprises the majority of this section.

The first step in the algorithm is to make an initial guess of the control profile ($U^{(0)}(t)$) over time. The problem is developed such that this initial control profile is updated iteratively to converge to the desired control profile (i.e. $U^*(t) = U^{(iter_{max})}(t)$ where $iter_{max}$ is the maximum iteration number). For any iteration ($iter$), the control input $U^{(iter)}(t)$ is also referred to as the nominal control input and is represented as $\overline{U}(t)$.

The second step is to determine the nominal state trajectories ($\overline{\boldsymbol{X}}(t)$) corresponding to $\overline{U}(t)$. This is done by simulating the system in equation (25) with the control $\overline{U}(t)$. In this step, the system in equation (25) is also linearized to get the error dynamics as

$$\boldsymbol{\Delta \dot{X}} = \left.\frac{\partial \boldsymbol{F}}{\partial \boldsymbol{X}}\right|_{\boldsymbol{X}=\overline{\boldsymbol{X}},U=\overline{U}} \boldsymbol{\Delta X} + \left.\frac{\partial \boldsymbol{F}}{\partial U}\right|_{\boldsymbol{X}=\overline{\boldsymbol{X}},U=\overline{U}} \Delta U. \tag{33}$$

The third step is to discretize this linear system so that the problem in the discrete domain becomes tractable. The discretized

version of equation (33) assuming a Zero Order Hold setting can be written as

$$\Delta \boldsymbol{X}(k+1) = G_k \Delta \boldsymbol{X}(k) + H_k \Delta U(k) \tag{34}$$

where k is the k^{th} time step, G_k and H_k are state dependent discretized system matrices. Equation (34) can be simplified to

$$\Delta \boldsymbol{X}(k+1) = \left(\prod_{j=0}^{k} G_j \right) \Delta \boldsymbol{X}(0) + H_k \Delta U(k) + \sum_{j=0}^{k-1} \left(\prod_{m=j+1}^{k} G_m \right) H_j \Delta U(j) \tag{35}$$

where $\Delta \boldsymbol{X}(0)$ represents the initial perturbation state of each trajectory and is equal to 0.

For the entire work, the simulation time has been assumed to be $T_f = 250\,min$ and the sampling time to be $T_s = 1\,min$. This makes k vary between 0 and 249. Correspondingly, the number of inputs is 250, i.e. $U(0)$ through $U(249)$. If the entire control profile is defined by the vector $\boldsymbol{U} = [U(0), U(1), \ldots, U(249)]^T$, the entire blood glucose profile by $\hat{\boldsymbol{G}} = [\hat{G}(1), \hat{G}(2), \ldots, \hat{G}(250)]^T$), the glucose error dynamics can be given by the equation

$$\Delta \hat{\boldsymbol{G}} = M \Delta \boldsymbol{U} \tag{36}$$

where $M =$

$$\begin{bmatrix} C_{glu} H_0^{(i)} & \cdots & \\ C_{glu} G_1^{(i)} H_0^{(i)} & C_{glu} H_1^{(i)} & \\ \vdots & \vdots & \ddots \\ C_{glu} \left(\prod_{j=1}^{k} G_j^{(i)} \right) H_0^{(i)} & \cdots & \cdots \; C_{glu} H_{249}^{(i)} \end{bmatrix} \tag{37}$$

and $C_{glu} = [\Psi, 0, 0]$. Thus, equation (36) allows us to write the blood glucose perturbation as a linear function of the input perturbation.

C_{glu} can also be used to write the nominal blood glucose trajectory as

$$\overline{\hat{\boldsymbol{G}}} = E[C_{glu}] \boldsymbol{X} \tag{38}$$

where $E[C_{glu}] = [M_{mean}, 0, 0]$. Therefore, the blood glucose profile $\hat{\boldsymbol{G}}$ due to a $\Delta \boldsymbol{U}$ change in the control input profile $\overline{\boldsymbol{U}}$ can be finally written as

$$\hat{\boldsymbol{G}} = \overline{\hat{\boldsymbol{G}}} + \Delta \hat{\boldsymbol{G}} \tag{39}$$

where $\overline{\hat{\boldsymbol{G}}}$ is the stochastic nominal blood glucose trajectory due to the control input $\overline{\boldsymbol{U}}$ and $\Delta \hat{\boldsymbol{G}}$ is the stochastic perturbation about $\overline{\hat{\boldsymbol{G}}}$ due to a perturbation in the control input $\Delta \boldsymbol{U}$.

Once, an expression to evaluate the blood glucose profile is available (equation (39)), a cost function can be posed which conceptually is equivalent to the cost in the optimization problem $P1$. Since, we want to minimize the error between the mean blood glucose of a type 1 diabetic patient and that of a target trajectory, we define a new cost function

$$J = ||E[\hat{\boldsymbol{G}}] - \boldsymbol{G}_{target}||_2 \tag{40}$$

where $\boldsymbol{G}_{target} = [G_{target}(1), \ldots, G_{target}(250)]^T$. Now that the cost function is developed, the next procedure is to enforce the desired constraints on the blood glucose concentration.

As was mentioned previously, the goal was to determine a control profile such that no realization of the stochastic system violated the constraints. Bernstein bounds allow us to pose these constraints (albeit conservatively) effectively. The constraints that need to be enforced are

$$min[\hat{G}(k)] \geq G_{dlb} \text{ for } k = 0, \ldots, 249 \tag{41}$$

$$max[\hat{G}(k)] \leq G_{ulb} \text{ for } k = t_m + 120, \ldots, 250 \tag{42}$$

where $\hat{G}(k)$ is the value of the stochastic glucose state at the k^{th} time step and therefore the k^{th} element of the vector $\hat{\boldsymbol{G}}$. Using relation (39), inequality (41) can be approximated as

$$min[\overline{\hat{G}}(k) + \Delta \hat{G}(k)] \geq G_{dlb} \tag{43}$$

$$\Rightarrow \overline{\hat{G}}(k) + min[\Delta \hat{G}(k)] \geq G_{dlb} \tag{44}$$

The reader should now note that $\Delta \hat{G}(k)$ is the k^{th} element of the vector $\Delta \hat{\boldsymbol{G}}$ making $\Delta \hat{G}(k) = M_k \Delta \boldsymbol{U}$ where M_k is the k^{th} row of M. On observing M_k carefully, we can write the inequality (44) as

$$\overline{\hat{G}}(k) + min[M_k \Delta \boldsymbol{U}] \geq G_{dlb} \tag{45}$$

$$\Rightarrow \overline{\hat{G}}(k) + min[C_{glu} \Delta \boldsymbol{X}(k)] \geq G_{dlb} \tag{46}$$

$$\Rightarrow \overline{\hat{G}}(k) + min[\Psi \Delta \boldsymbol{X}_{\boldsymbol{G}}(k)] \geq G_{dlb}. \tag{47}$$

Since, $\Psi \Delta \boldsymbol{X}_{\boldsymbol{G}}(k)$ is a polynomial function with Bernstein polynomials as their bases, the range enclosing property can be used to determine the minimum of the polynomial as

$$\overline{\hat{G}}(k) + min[\Delta x_0(k), \ldots, \Delta x_N(k)] \geq G_{dlb}. \tag{48}$$

Satisfying inequality (48) is now equivalent to satisfying the $N+1$ inequalities

$$\begin{aligned} &\overline{\hat{G}}(k) + \Delta x_i(k) \geq G_{dlb} \\ &\qquad \text{for } i = 0, \ldots, N \text{ and } \forall k. \end{aligned} \tag{49}$$

Hence, now the original hypoglycemic non-linear constraint in $P1$ at any instant in time can be approximated by $N+1$ linear constraints (equation (49)). Similarly, the original hyperglycemic constraint at any instant in time in $P1$ can also be approximated by the $N+1$ linear constraints

$$\begin{aligned} &\overline{\hat{G}}(k) + \Delta x_i(k) \leq G_{dub} \\ &\qquad \text{for } i = 0, \ldots, N \text{ and for } k = t_m + 120, \ldots, 250. \end{aligned} \tag{50}$$

The fourth step in the algorithm is to finally solve the following optimization problem ($P2$)

$$\begin{aligned} \text{minimize}_{\Delta \boldsymbol{U}} \quad & J \\ \text{subject to} \quad & \overline{\hat{G}}(k) + \Delta x_i(k) \geq G_{dlb} \\ & \quad \text{for } i = 0, \ldots, N \text{ and } \forall k \\ & \overline{\hat{G}}(k) + \Delta x_i(k) \leq G_{dub} \\ & \quad \text{for } i = 0, \ldots, N \\ & \quad \text{and for } k = t_m + 120, \ldots, 250 \\ & \overline{U} + \Delta \boldsymbol{U} \geqslant 0. \end{aligned} \tag{51}$$

Once the solution to $P2$ (i.e. $\Delta \boldsymbol{U}^*$) is obtained, the control input solution is updated using the relation

$$\boldsymbol{U}^{*(iter+1)} = \overline{\boldsymbol{U}} + \Delta \boldsymbol{U}^* \tag{52}$$

and the process is repeated all the way from step one. As the entire control problem is resolved by solving convex quadratic optimizations ($P2$) sequentially at each iteration, the phrase Sequential Quadratic Programming (SQP) is used to justify the title of the paper.

Results from the SQP are now presented. The SQP algorithm is started with an initial nominal guess for the control. The initial control guess is assumed to be all zeros, i.e. $\boldsymbol{U}^{(0)} = [0, 0, \ldots, 0]^T$.

It should be pointed out that the optimization assumes a linear approximation of the true non-linear model. Therefore finding a control solution for the linearized model which satisfies all the constraints does not imply that the same control on the true system would also satisfy those constraints. Hence, the SQP algorithm is terminated only if it is observed that the control solution is able to satisfy all the constraints even for the true nonlinear system. In the illustrated case, the SQP algorithm is terminated at the 20^{th} iteration. The control solution obtained at the end of the 20^{th} iteration is shown in Figure 3. The associated glucose variation is shown in Figure 4. In this figure we see that the glucose variation lies well within the determined Bernstein bounds as well as showing all the MC realization satisfying the desired hypoglycemic and hyperglycemic constraints (presenting the success of the SQP algorithm).

It is interesting to note that $E[\hat{G}(t)]$ is pretty far away from the blue target trajectory in the first half of the simulation (i.e. for $t < 100\,min$). This is because the lower bound on the glucose (determined using the Bernstein Range Enclosing property) is tightly pressed against the desired hypoglycemic lower bound. If additional insulin was administered to lower the yellow curve towards the blue one, the lower black curve would end up violating the acceptable lower glucose level (G_{dlb}). However, the optimizer does the best it can: as is evident in the later half of the plot where the tracking performance is much better (since none of the black curves are close to being active, i.e. none of the hypo or the hyperglycemic constraints are active).

It should also be mentioned that although the optimization problem being solved is a convex one, the final solution obtained need not be globally optimal. This is because the optimization problem tries to determine a perturbation profile about a preestablished control trajectory and not estimate the entire control input. Therefore, the optimization problem posed in this section only provides the best perturbation profile. Repeatedly solving this optimization problem (by updating the nominal control input) however, allows us to converge to a reasonable solution. It must also be mentioned that for an assumed $\overline{\boldsymbol{U}}$, a solution might not be feasible. This does not mean that a control input solution does not exist, but it just motivates the algorithm to select a better $\overline{\boldsymbol{U}}$.

6 CONCLUSIONS

A Bernstein bound based approach for the design of insulin profiles to regulate blood glucose in Type 1 diabetic patients is studied. A sequential quadratic programming approach is used to design a controller for a model for Type 1 diabetes with uncertainties in meal size and initial blood glucose. Numerical results are encouraging to warrant studying more complex models such as gut dynamics and including subcutaneous insulin infusion as well.

ACKNOWLEDGMENT

This material is based upon work supported through National Science Foundation (NSF) under Awards No. CMMI-1537210.

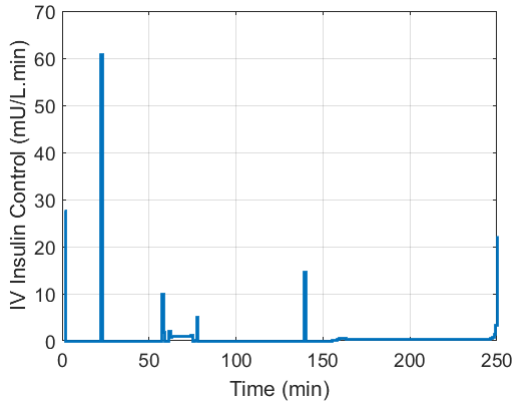

FIGURE 3. Control Solution $\boldsymbol{U}*$ obtained after 20 iterations of the SQP

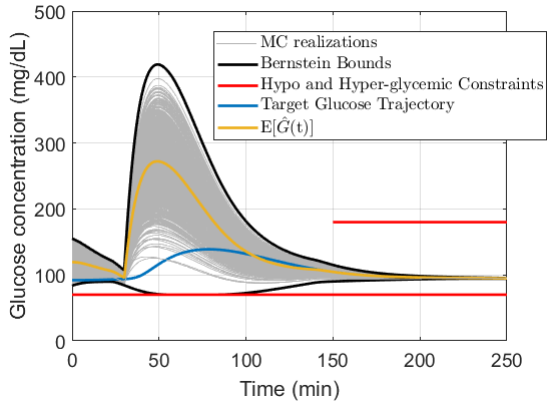

FIGURE 4. Variation of the Stochastic Glucose state under the influence of $\boldsymbol{U}*$

REFERENCES

[1] for Disease Control, C., Prevention, et al., 2017. "National diabetes statistics report, 2017". *Atlanta, GA: Centers for Disease Control and Prevention, US Department of Health and Human Services*.

[2] Organization, W. H., et al., 2016. *Global report on diabetes*. World Health Organization.

[3] Cryer, P. E., 2007. "Hypoglycemia, functional brain failure, and brain death". *The Journal of clinical investigation,* ***117***(4), pp. 868–870.

[4] Cobelli, C., Renard, E., and Kovatchev, B., 2011. "Artificial pancreas: past, present, future". *Diabetes,* ***60***(11), pp. 2672–2682.

[5] Heinemann, L., Benesch, C., DeVries, J. H., home consortium, A., et al., 2011. "Ap@ home: a novel european approach to bring the artificial pancreas home". *Journal of diabetes science and technology,* ***5***(6), pp. 1363–1372.

[6] Russell, S. J., El-Khatib, F. H., Sinha, M., Magyar, K. L., McKeon, K., Goergen, L. G., Balliro, C., Hillard, M. A., Nathan, D. M., and Damiano, E. R., 2014. "Outpatient glycemic control with a bionic pancreas in type 1 diabetes". *New England Journal of Medicine,* ***371***(4), pp. 313–325.

[7] Dassau, E., Bequette, B. W., Buckingham, B. A., and Doyle, F. J., 2008. "Detection of a meal using continuous glucose monitoring implications for an artificial β-cell". *Diabetes care,* ***31***(2), pp. 295–300.

[8] Lunze, K., Singh, T., Walter, M., Brendel, M. D., and Leonhardt, S., 2013. "Blood glucose control algorithms for type 1 diabetic patients: A methodological review". *Biomedical Signal Processing and Control,* ***8***(2), pp. 107–119.

[9] Chen, S., Weimer, J., Rickels, M. R., Peleckis, A., and Lee, I., 2015. "Towards a model-based meal detector for type i diabetics". In 6th Workshop on Medical Cyber-Physical Systems.

[10] Bergman, R. N., Phillips, L. S., and Cobelli, C., 1981. "Physiologic evaluation of factors controlling glucose tolerance in man: measurement of insulin sensitivity and beta-cell glucose sensitivity from the response to intravenous glucose.". *Journal of Clinical Investigation,* ***68***(6), p. 1456.

[11] Fisher, M. E., 1991. "A semiclosed-loop algorithm for the control of blood glucose levels in diabetics". *IEEE transactions on biomedical engineering,* ***38***(1), pp. 57–61.

[12] Dalla Man, C., Camilleri, M., and Cobelli, C., 2006. "A system model of oral glucose absorption: validation on gold standard data". *IEEE Transactions on Biomedical Engineering,* ***53***(12), pp. 2472–2478.

[13] Pacini, G., and Bergman, R. N., 1986. "Minmod: a computer program to calculate insulin sensitivity and pancreatic responsivity from the frequently sampled intravenous glucose tolerance test". *Computer methods and programs in biomedicine,* ***23***(2), pp. 113–122.

[14] Dalla Man, C., Rizza, R. A., and Cobelli, C., 2007. "Meal simulation model of the glucose-insulin system". *IEEE Transactions on Biomedical Engineering,* ***54***(10), pp. 1740–1749.

[15] Lynch, S. M., and Bequette, B. W., 2002. "Model predictive control of blood glucose in type I diabetics using subcutaneous glucose measurements". In Proceedings of the American Control Conference, pp. 4039–4043.

[16] US Department of Agriculture, U. D. o. H., and Services, H., 2010. Dietary guidelines for americans, 2010.

[17] Association, A. D. Carbohydrate counting. http://www.diabetes.org/food-and-fitness/food/what-can-i-eat/understanding-carbohydrates/carbohydrate-counting.html. Accessed: 2016-08-17.

[18] Nandi, S., Singh, T., Mastrandrea, L. D., and Singla, P., 2017. "Optimal meal time after bolusing for type 1 diabetes patients under meal uncertainties". In American Control Conference (ACC), 2017, IEEE, pp. 4412–4417.

[19] Garloff, J., 2003. "The Bernstein expansion and its applications".
[20] Ray, S., and Nataraj, P., 2009. "An efficient algorithm for range computation of polynomials using the bernstein form". *Journal of Global Optimization,* ***45***(3), pp. 403–426.
[21] Seaquist, E. R., Anderson, J., Childs, B., Cryer, P., Dagogo-Jack, S., Fish, L., Heller, S. R., Rodriguez, H., Rosenzweig, J., and Vigersky, R., 2013. "Hypoglycemia and diabetes: A report of a workgroup of the american diabetes association and the endocrine society". *Diabetes Care,* ***36***(5), pp. 1384–1395.
[22] Association, A. D. Checking your blood glucose. http://www.diabetes.org/living-with-diabetes/treatment-and-care/blood-glucose-control/checking-your-blood-glucose.html. Accessed: 2016-08-18.

Appendix

The Bergman Model used for generating the target trajectory was

$$\dot{G}(t) = -(X(t)+p_1)G(t) + p_1 G_b + R_{ag}(t)/V_g \tag{53}$$

$$\dot{X}(t) = -p_2 X(t) + p_3(I(t)-I_b) \tag{54}$$

$$\dot{I}(t) = -p_4 I(t) + \gamma(G(t)-h)(t-t_m) \tag{55}$$

where V_g (dL) is the distribution volume of glucose. The initial conditions for the trajectory was selected as

$$G(0) = G_b;\ X(0) = 0;\ \text{and}\ I(0) = I_b.$$

The additional term $R_{ag}(t)$ (mg) (also referred to as the Rate of appearance of glucose in plasma) is introduced in the model to replicate a meal intake disturbance. In this work, the dynamics that determine $R_{ag}(t)$ is evaluated from a gut dynamics model adopted from [12]. The model is given by the equations

$$\dot{q}_{sto1}(t) = -k_{21} q_{sto1}(t) + D\delta(t-t_m) \tag{56}$$

$$\dot{q}_{sto2}(t) = -k_{empt} q_{sto2}(t) + k_{21} q_{sto1}(t) \tag{57}$$

$$\dot{q}_{gut}(t) = -k_{abs} q_{gut}(t) + k_{empt} q_{sto2}(t) \tag{58}$$

$$R_{ag}(t) = f k_{abs} q_{gut}(t) \tag{59}$$

$$q_{sto} = q_{sto1} + q_{sto2} \tag{60}$$

$$k_{empt}(q_{sto}) = k_{min} + 0.5(k_{max}-k_{min})(\tanh[\alpha(q_{sto} - bD)] - \tanh[\beta(q_{sto}-cD)] + 2) \tag{61}$$

$$\alpha = \frac{5}{2D(1-b)} \tag{62}$$

$$\beta = \frac{5}{2Dc}. \tag{63}$$

where q_{sto1} (mg) and q_{sto2} (mg) are the amounts of glucose in solid and liquid phases respectively present in the stomach at any time. q_{gut} (mg) is the amount of glucose in the intestines, $\delta(.)$ is the Dirac delta function and D (mg) is the amount of glucose consumed during the meal. In this work D was assumed to be 45000 to correspond to a 45 gr CHO meal. k_{21} (min^{-1}) is a constant which determines the rate at which food moves from the first stomach state to the second. k_{empt} (min^{-1}) represents the rate at which the food is drained from the second stomach state to the gut state. It is bounded by maximum and minimum values k_{max} and k_{min} respectively. k_{abs} (min^{-1}) is the rate at which the carbohydrates are absorbed into the body from the gut. α and β are parameters which determine the transition of k_{empt} between its extremities. Finally, b, c and f are other dimensionless parameters of the model.

All the parameters needed to generate the target trajectory have been listed in Table 2.

TABLE 2. Parameter values for a normal subject

Parameter	Value	Parameter	Value
p_1	0.03082	k_{max}	0.0558
p_2	0.02093	k_{min}	0.0080
p_3	1.062×10^{-5}	k_{abs}	0.057
p_4	0.30000	k_{21}	0.0558
γ	0.003349	b	0.82
h	89.5	c	0.00236
G_b	92	f	0.9
I_b	7.3	V_g	146.64